

## MYOTOMAL MUSCLE FUNCTION AT DIFFERENT LOCATIONS IN THE BODY OF A SWIMMING FISH

J. D. ALTRINGHAM<sup>1</sup>, C. S. WARDLE<sup>2</sup> AND C. I. SMITH<sup>1</sup>

<sup>1</sup>*Department of Pure and Applied Biology, The University, Leeds LS2 9JT, UK and*

<sup>2</sup>*SOAFD, Marine Laboratory, PO Box 101, Aberdeen AB9 8DB, UK*

*Accepted 4 May 1993*

### Summary

We describe experiments on isolated, live muscle fibres which simulate their *in vivo* activity in a swimming saithe (*Pollachius virens*). Superficial fast muscle fibres isolated from points 0.35, 0.5 and 0.65 bodylengths (BL) from the anterior tip had different contractile properties. Twitch contraction time increased from rostral to caudal myotomes and power output (measured by the work loop technique) decreased. Power *versus* cycle frequency curves of rostral fibres were shifted to higher frequencies relative to those of caudal fibres. In the fish, phase differences between caudally travelling waves of muscle activation and fish bending suggest a change in muscle function along the body. *In vitro* experiments indicate that *in vivo* superficial fast fibres of rostral myotomes are operating under conditions that yield maximum power output. Caudal myotomes are active as they are lengthened *in vivo* and initially operate under conditions which maximise their stiffness, before entering a positive power-generating phase. A description is presented for the generation of thrust at the tail blade by the superficial, fast, lateral muscle. Power generated rostrally is transmitted to the tail by stiffened muscle placed more caudally. A transition zone between power generation and stiffening travels caudally, and all but the most caudal myotomes generate power at some phase of the tailbeat. Rostral power output, caudal force, bending moment and force at the tail blade are all maximal at essentially the same moment in the tailbeat cycle, as the tail blade crosses the swimming track.

### Introduction

Carangiform fish swim using lateral oscillations of the body, with most of the thrust coming from the blade of the caudal fin (Lighthill, 1971). Steady swimming speed increases with increased tailbeat frequency and with the recruitment of more fibres within the lateral muscle, but patterns of body movement and muscle activation remain essentially constant (Hess and Videler, 1984; Videler and Hess, 1984; van Leeuwen *et al.* 1990; Wardle and Videler, 1993). How force developed by the lateral muscle is converted to thrust at the tail is still uncertain. Recent kinematic and electromyographical (EMG) studies (Hess and Videler, 1984; Williams *et al.* 1989; van Leeuwen *et al.* 1990; Wardle and Videler, 1993)

Key words: fish, *Pollachius virens*, mechanics, muscle, power output, swimming.

provide a description of muscle strain and activation cycles during swimming. Data are particularly extensive for the saithe (*Pollachius virens*), a fast pelagic swimmer (Hess and Videler, 1984; Wardle and Videler, 1993). In steady swimming, waves of body curvature travel down the fish. The strain (length change) cycle of superficial lateral muscle is essentially sinusoidal. Waves of muscle activation, alternating from left to right sides, travel faster than those of body curvature, leading to systematic phase differences between strain and activation cycles along the body, suggesting a change in muscle function. EMG activity in rostral (towards the head) myotomes is recorded primarily during muscle shortening and in caudal myotomes during both lengthening and shortening. The behaviour of myotomal muscle at different locations on the trunk in carp has been mathematically modelled by van Leeuwen *et al.* (1990), but no direct measurements of muscle function have been made under these conditions. Twitch contraction time of fast myotomal muscle blocks increases towards the tail in several teleost species (Wardle *et al.* 1989). No hypotheses have been put forward to explain this observation, nor has it been confirmed on isolated fibres. In this paper we describe experiments in which conditions approximating to those *in vivo* have been imposed on isolated, superficial fast muscle fibres from three locations in saithe (*Pollachius virens*), using the kinematic and EMG data of Wardle and Videler (1993). An explanation is given of how this muscle may contribute to the generation of thrust at the tail blade, based on the results of these experiments.

### Materials and methods

All experiments were carried out at the SOAFD Marine Laboratory Field Station, Aultbea, Loch Ewe, Wester Ross, Scotland, in July 1991 and July 1992. Saithe 24–29 cm in length were caught on hand lines from a boat using barbless hooks, placed in large plastic bins and quickly transferred to a 10m tank at 12°C (seawater temperature in Loch Ewe). Fish were used within a few days of capture. Bundles of fast myotomal muscles were isolated and studied using methods previously described (Altringham and Johnston, 1990*a,b*). Fast fibres were chosen for the following reasons: Johnston and Moon (1980) found that superficial fast fibres were recruited at around 5Hz in saithe of a similar size, during steady swimming, at sustainable speeds. The frequency range over which the fast fibres contribute to locomotion is greater than that for slow fibres. Over the frequency range studied by Wardle and Videler (1993), it is the fast fibres that are primarily active, and these results are the basis of some of our work. Fast fibres were studied from positions 5mm ventral to the lateral line in identified myotomes, 0.35 (rostral), 0.5 (mid) and 0.65 (caudal) body lengths (BL) from the rostral tip. The fibres used were located very close to the skin, immediately below the slow fibres and had the same orientation – parallel (within approximately 10°) to the skin and the long axis of the body. To ensure that any pink fibres from the very thin intermediate layer (Johnston and Moon, 1980) were not included, several more fibre layers were removed, and only large-diameter transparent fibres were selected. The fibres were attached to the apparatus by clipping a trimmed section of the connective tissue layer directly beneath the skin, which is continuous with the myosepta at each end of the myotome. Bundles of 5–20 fibres were stable for many hours at 12°C. At

the start of each experiment, fibre length ( $l_0$ ) was adjusted to yield a maximal twitch with a supramaximal stimulus. This corresponded closely to the resting length in the fish when lying flat on the bench. At this length, resting force was typically around 1–3% of maximal tetanic force. The stimulation frequency eliciting a maximal isometric tetanus was then established, and this was used in subsequent oscillatory work experiments. Maximum oscillatory power output could not be increased by changing stimulation frequency. *In vivo*, superficial myotomal muscle undergoes essentially sinusoidal length changes (strains) and is active during part of each cycle. This pattern can be simulated on isolated fibres using the work loop or oscillatory work technique (Josephson, 1985). At 8 min intervals, preparations were subjected typically to eight sinusoidal strain oscillations and stimulated phasically in each cycle. Strain amplitude and the number and timing of stimuli were manipulated as described below to approximate *in vivo* conditions. Work and power were calculated using the work loop technique (Josephson, 1985; Altringham and Johnston, 1990a,b). Work per cycle typically declined by 0–3% per cycle during a run, but recovery was complete between runs. Power outputs were calculated from the work performed in cycle 3, having first established that this method gave results comparable to those from the mean of the first six cycles.

## Results

### *Isometric mechanical properties and power output using work loops*

These results are summarised in Table 1. Isometric twitch contraction time, measured as time to peak force ( $t_a$ ) and time from stimulus to 90% relaxation ( $t_{90}$ ), increased

Table 1. Summary of mechanical properties of fast muscle fibres from three locations on the body of a saithe, 0.35, 0.5 and 0.65 bodylengths (BL) from the rostral tip

Mechanical property	Muscle location		
	0.35BL	0.5BL	0.65BL
Time to peak force, $t_a$ (ms)	27±0.7 (7)	33±0.8 (5)	44±0.9 (8)
Time from stimulus to 90% relaxation, $t_{90}$ (ms)	62±5 (7)	69±5 (5)	136±10 (8)
Tetanic fusion frequency (Hz)	70	60	40
Maximal isometric tension, $P_0$ (kNm <sup>-2</sup> )	147±25 (6)	151±15 (5)	136±19 (6)
Maximum power output (Wkg <sup>-1</sup> ) at a strain of ±5% $l_0$	63±13 (6)	56±8 (5)	31±8 (4)

All values are mean ± s.e. ( $N$ , number of observations).

Statistical analysis using ANOVA revealed the following. Mean  $t_a$  for muscle from each location was significantly different from that of the muscles at the other two locations ( $P<0.01$ ). Mean  $t_{90}$  for muscle from 0.65BL was significantly different from that from 0.35 and 0.50BL ( $P<0.01$ ). Mean power output from muscle from 0.65BL was significantly different from that from 0.35 and 0.50BL ( $P<0.05$ ). All other differences were not significant at the 5% level. Tetanic fusion frequencies were not determined precisely and not tested statistically.

$l_0$ , fibre length for maximal twitch.

significantly in a rostral to caudal direction. Tetanic fusion frequencies decreased in a rostral to caudal direction. Maximum isometric tensions were not significantly different between the three locations, although almost so between 0.50 and 0.65BL ( $P=0.051$ ). Maximum power output was determined over a range of cycle frequencies, at a strain amplitude of  $\pm 5\%$   $l_0$  (10% peak-to-peak about  $l_0$ ), by systematically changing the number and timing of stimuli. Moving from rostral to caudal locations, the power *versus* cycle frequency curves were shifted to lower frequencies (Fig. 1). When power output was normalised to the maximum at 8Hz, power outputs of 0.35 and 0.65BL preparations were significantly different at all other frequencies ( $P<0.01$ , Mann–Whitney test). Values for 0.5BL preparations were intermediate, but not always significantly different from those of 0.35 and 0.65BL. Absolute power output ( $\text{Wkg}^{-1}$ ) of caudal myotomal preparations was significantly lower than at the other two locations ( $P<0.05$ ).

The aim of subsequent experiments was to mimic, as closely as current knowledge allowed, the behaviour of myotomal muscle *in vivo* during swimming. We have used the term *swimming simulations* to describe these experiments, for want of a more descriptive yet short term, but appreciate that at this stage the simulations can only be approximate.

### Swimming simulations

#### Rostral myotomes

We have used estimated strain amplitudes for superficial muscles, as calculated by Hess and Videler (1984) for the saithe. Deeper fast fibres have been shown to undergo smaller strains (Rome and Sosnicki, 1991), in agreement with predictions made by Alexander (1969), but no measurements have been made on fast fibres as close to the

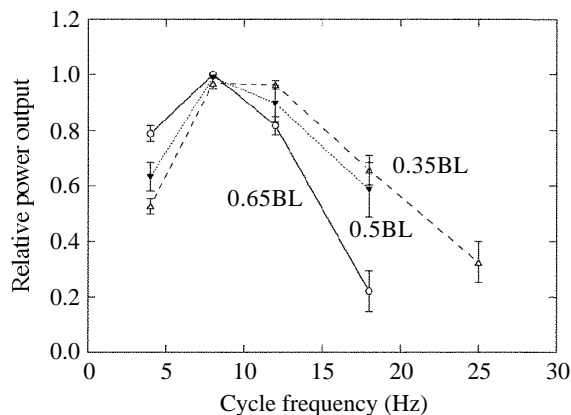


Fig. 1. Relative power output (normalised to maximum at 8Hz) plotted against cycle frequency at 12°C. Pooled data from myotomes 0.35, 0.5 and 0.65body lengths (BL) from the rostral tip. Points are mean  $\pm$  s.e. ( $N=6$ , 5 and 6, respectively). At each frequency, power output was maximised by systematically changing the number of stimuli in each cycle and their timing relative to the strain cycle. Power outputs of rostral (0.35BL) and caudal (0.65BL) muscle are significantly different ( $P<0.01$ ) at 4, 12 and 18Hz (Mann–Whitney test). The only significant differences between the power outputs of middle (0.5BL) and caudal muscle were at 5 and 18Hz.

surface as those used in the present study. Their position, orientation and firm attachment to the skin suggest to us that the strains estimated by Hess and Videler are the most appropriate. Strain amplitude of superficial fibres in saithe at 0.35 BL (rostral) was therefore assumed to be  $\pm 3\%$   $l_0$  during steady swimming (Hess and Videler, 1984). Maximum power output of isolated fibres from this location, at all cycle frequencies, was obtained when the first stimulus was given at a phase shift of  $30\text{--}40^\circ$  (1 cycle= $360^\circ$ ;  $0^\circ$ =muscle lengthening through  $l_0$ ) (Figs 2 and 3). This is the same phase shift observed between the strain cycle and the onset of EMG activity in a swimming fish at all tailbeat frequencies (Wardle and Videler, 1993). The duration of the EMG burst is a constant proportion of the tailbeat cycle, occupying  $160^\circ$  ( $40\text{--}200^\circ$ ) in rostral myotomes (Wardle and Videler, 1993). To obtain maximum power output, the duration of stimulation in isolated preparations was also an essentially constant proportion of the cycle period, at about  $100\text{--}130^\circ$  (see Fig. 2). Electrical activity would be recorded in the muscle after the last stimulus, giving an active period comparable to the *in vivo* EMG duration of  $160^\circ$ . Under these conditions, almost all force generation occurred during the shortening phase of the cycle, and the muscle therefore performed largely positive work (see Figs 5B, 6 and 7, discussed in detail below).

#### Caudal myotomes

Caudal myotomes (0.65BL) operate under very different conditions to rostral myotomes *in vivo*. At all tailbeat frequencies, muscle strain amplitude was estimated to be  $\pm 6\%$   $l_0$  (Hess and Videler, 1984), the phase shift for the onset of EMG activity is  $350^\circ$  and EMG burst duration is  $100^\circ$  ( $350\text{--}90^\circ$ ) (Wardle and Videler, 1993). Muscle is activated when shorter than  $l_0$  and, in the *in vitro* simulations, all of the rising phase of

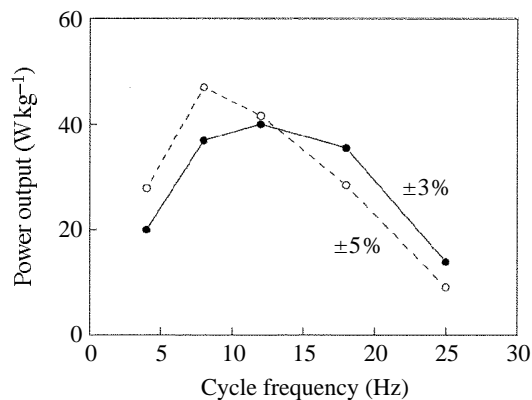


Fig. 2. Maximum mean power output plotted against cycle frequency for a representative rostral (0.35BL) preparation, at strain amplitudes of  $\pm 3\%$  (filled circles) and  $\pm 5\%$  (open circles) mean length in the body ( $l_0$ ). Strains were alternated at each frequency, and controls at 8 Hz were repeated at intervals. In all experiments, the optimum phase shift for the first stimulus was  $30\text{--}40^\circ$ . 7–8, 4, 2–3, 1 and 1 stimuli were delivered in each cycle (at 70 Hz) at cycle frequencies of 4, 8, 12, 18 and 25 Hz, respectively.

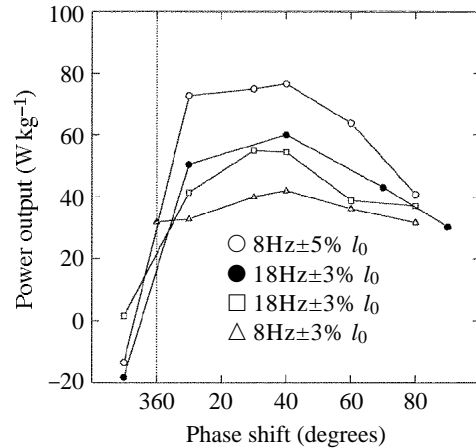


Fig. 3. Mean power output plotted against phase shift for a number of typical rostral (0.35BL) preparations. Values against each curve cycle refer to frequency and strain. At a cycle frequency of 8Hz, four stimuli per cycle were given at a frequency of 70Hz; at 18Hz, one stimulus was given per cycle.

force generation occurred when the muscle was being stretched (see Figs 5, 6 and 7, and see below for a detailed description). Muscle stiffness was maximal under these conditions (relative to that at other stimulus phase shifts), exerting forces  $1.75 \pm 0.06$  ( $N=6$ ) times greater than at a phase shift of  $30-40^\circ$  at a cycle frequency of 18Hz (compare forces at  $330/350^\circ$  with those at  $30^\circ$  in Fig. 4). The magnitude of the extra force recruited was dependent on cycle frequency, falling to a 1.5-fold increase at 8Hz.

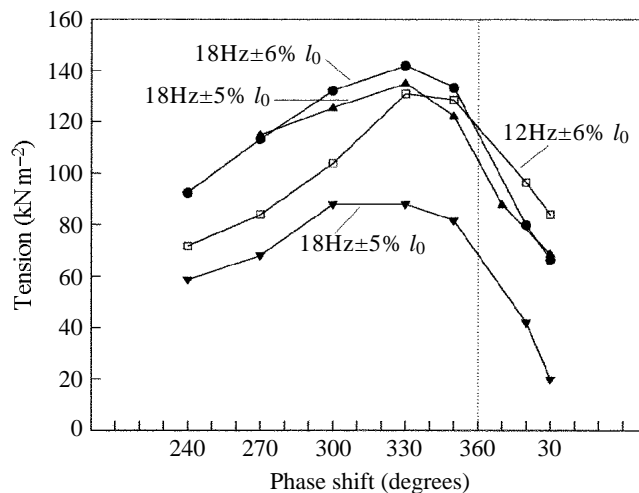


Fig. 4. Tension plotted against phase shift for a number of caudal (0.65BL) preparations. Values against each curve refer to cycle frequency and strain. One stimulus per cycle was given at both frequencies.

## Mid-point myotomes

At the time of experimentation, no EMG/kinematic data were available for myotomes at this location. We therefore assumed that the *in vivo* stimulus phase would be midway between that of rostral and caudal myotomes, at around 10–20°, an assumption supported by data from other species (van Leeuwen *et al.* 1990). Muscle strain was estimated to be  $\pm 4.5\% l_0$  (Hess and Videler, 1984). Power was maximal at a phase shift of 0–30°, a phase range similar to that predicted to be used *in vivo*. There was a small but systematic increase in optimum phase with decreasing cycle frequency, from 0° at 18Hz to 30° at 4Hz. This was apparent in all preparations in which phase shift was investigated over

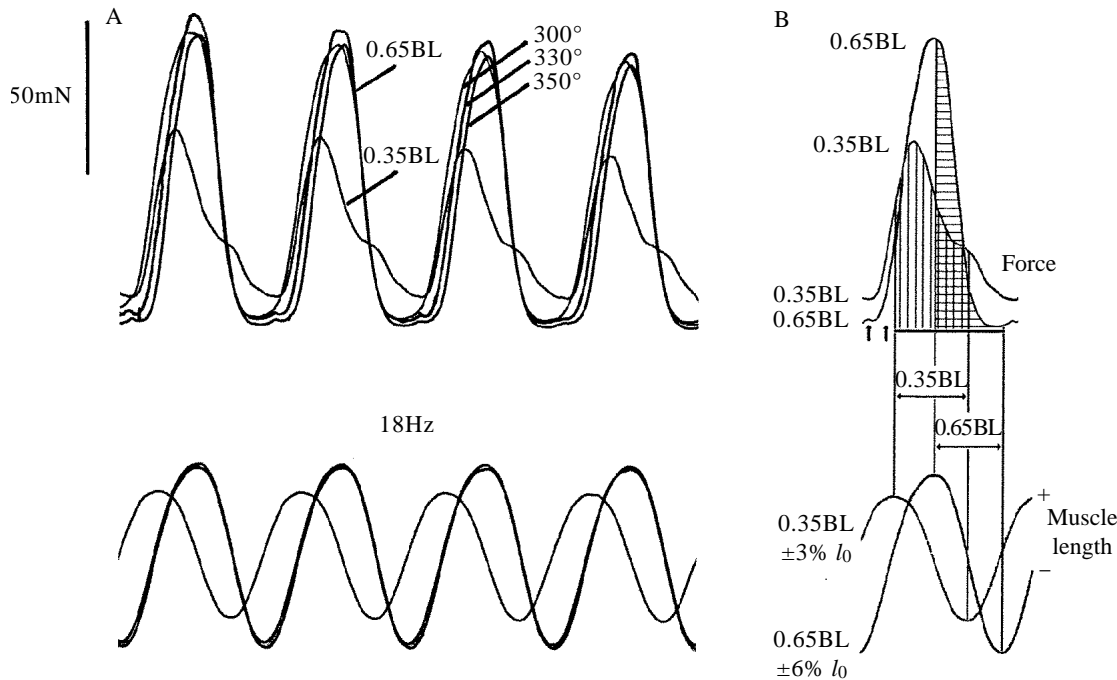


Fig. 5. (A) Muscle strain and force records of the middle four of eight oscillatory cycles. Records from two preparations from the same fish are shown, isolated from myotomes 0.35 and 0.65BL from the rostral tip. Strain and stimulation variables simulate the conditions predicted for steady-state swimming. The strain cycle at 0.65BL lags that at 0.35BL by 110°, as *in vivo*. 0.35BL, strain  $\pm 3\% l_0$ , one stimulus at 30°. 0.65BL, strain  $\pm 6\% l_0$ , one stimulus at 300, 330 and 350° for the three records shown: force is highest at 330°. Strain cycle frequency was 18Hz. The two preparations have different lengths and cross-sectional areas, and force and strain records have not been normalised to account for these differences. For further explanation refer to the text. (B) The fourth of eight cycles from other runs of the same two preparations. Vertical lines between the force and strain curves delineate shortening phases. The hatched areas indicate times during force generation when shortening is taking place, and the muscle is performing positive work. At 0.35BL, the muscle is shortening throughout most of the force-generating part of the cycle (vertical hatching), producing positive power. Over the same period, muscle at 0.65BL is initially stretched when active and only produces power late in its force-generating phase (horizontal hatching). Stimulus timing is indicated for 0.35BL (left arrow) and 0.65BL (right arrow) myotomes.

several frequencies (data not shown). This change in optimum phase shift is probably too small to have been detected by EMG/kinematic studies. These results suggest that, under *in vivo* conditions, muscle at 0.5BL generates largely positive work during the tailbeat.

#### Combining data from different locations on the body

Fig. 5 shows force and strain cycles for rostral and caudal preparations from the same fish. Strain and stimulation variables simulating those estimated for the *in vivo* situation were used (see above and figure legend). In the swimming fish, the waves of bending and EMG activity travel down the body in a caudal direction. The records from the more caudal preparation are therefore offset by  $110^\circ$  relative to those of the rostral preparation (Wardle and Videler, 1993) to take account of the delay. At 0.65BL, peak force was consistently obtained at a phase of  $330^\circ$  (Fig. 5A), rather than the  $350^\circ$  observed *in vivo* (Wardle and Videler, 1993). However, the *in vitro* relationship between power and stimulus phase shift has a broad peak (Figs 4 and 5A), and *in vivo* measurements were

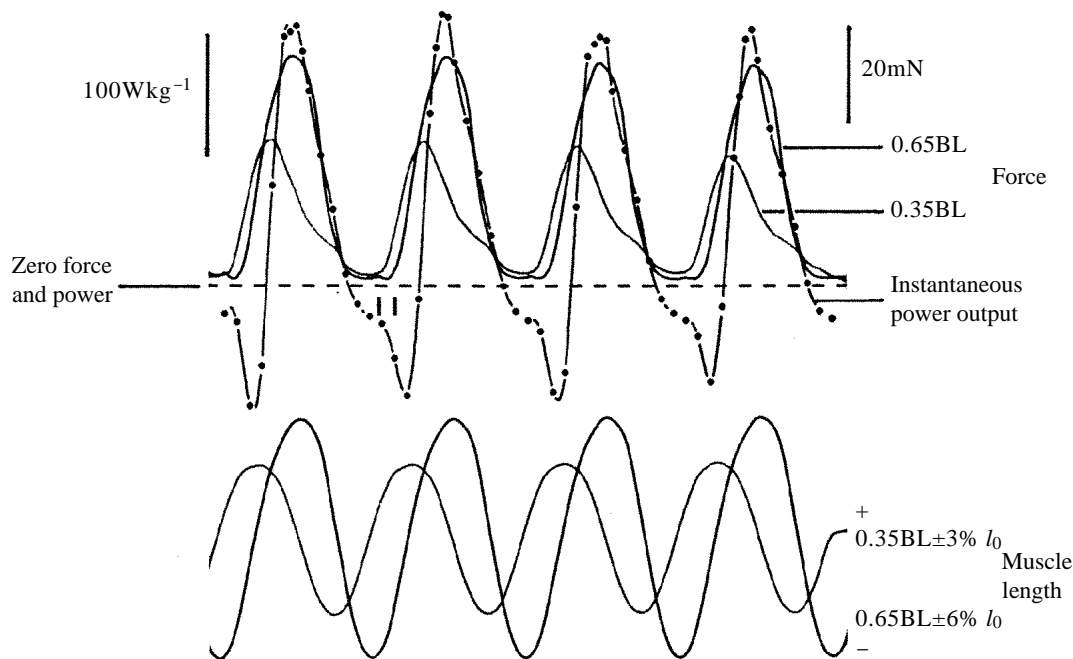


Fig. 6. Muscle strain and force records of the middle four of eight oscillatory cycles. Records from two preparations from a different fish from that of Fig. 5 are shown, isolated from myotomes 0.35 and 0.65BL from the rostral tip. Instantaneous power output of the 0.35BL preparation is also shown. Strain and stimulation variables simulate the conditions predicted for steady-state swimming, and strain cycle at 0.65BL lags that at 0.35BL by  $110^\circ$ , as *in vivo*: 0.35BL, strain  $\pm 3\% l_0$ , one stimulus at  $30^\circ$ ; 0.65BL, strain  $\pm 6\% l_0$ , one stimulus at  $330^\circ$ ; strain cycle frequency was 18Hz. For further explanation refer to the text. Note that peak power output at 0.35BL coincides with peak force at 0.65BL. The two preparations have different lengths and cross-sectional areas, and force and strain records have not been normalised to account for these differences. Stimulus timing is indicated for 0.35BL (left bar) and 0.65BL (right bar) myotomes in the second cycle.

subject to errors of a similar magnitude to this discrepancy. In Fig. 5B, vertically (0.35BL) and horizontally (0.65BL) hatched areas under force curves denote the portion of the cycle during which positive work is performed, i.e. during the shortening phase of the cycle, delineated by the vertical lines between the force and strain records. Note that the relative timing is important here, not (for the present discussion) absolute force. Preparations differed in cross-sectional area and length, and the records in Figs 5–7 have not been normalised for these differences.

A second example is shown in Fig. 6 from two preparations from a different fish, in which instantaneous power generated at 18Hz by the rostral myotomes has also been calculated from the force and strain results and is included on the plot. Peak power output of muscle from 0.35BL coincides with peak force of muscle from 0.65BL. Fig. 7A shows force and strain records from three preparations from three fish of the same length, at a cycle frequency of 12Hz, revealing a similar pattern to that observed at 18Hz. Strain cycles of 0.5BL and 0.65BL preparations lagged behind that of 0.35BL by 55° and 110°, respectively, as *in vivo* (Wardle and Videler, 1993), and each preparation was operating under predicted *in vivo* conditions (see legend, Fig. 7A). In Fig. 7B, instantaneous power output has been calculated for all three preparations over the middle two cycles. To enable comparisons to be made between sites, instantaneous power output has been corrected by multiplying it by  $P_0/xP_0$  (where  $P_0$  is isometric stress and  $xP_0$  is the mean stress for preparations from that location on the body). This resulted in minimal changes in power at 0.35/0.50BL and a 30% increase at 0.65BL. Thus, under predicted *in vivo* conditions, power peaks sequentially from rostral to caudal myotomes and, in the caudal region, positive power output is preceded by a period of negative work. In the caudal region, mean power output is close to zero.

## Discussion

### *Basic mechanical properties*

The increase in twitch contraction time from rostral to caudal myotomes has been recorded in several species from measurement of the contraction time of large blocks of myotomal muscle (e.g. Wardle, 1985). The decrease in power output towards the tail can be explained in part by the slowing of twitch kinetics. At a given frequency, more caudally placed myotomes will spend a greater proportion of the cycle at sub-maximal levels of activation. As cycle frequency increases, caudal fibres will be unable to relax fully before the lengthening phase of the cycle, and mean power output will decline. Maximum power output of the more rostral fibres is higher than any previously measured for fish muscle; that of caudal myotomes is comparable to values for sculpin and cod fast muscle fibres (Altringham and Johnston, 1990a; Moon *et al.* 1991). The higher experimental temperature, and the short twitch contraction times of rostral saithe muscle, will account for the high power output relative to that of other fish muscle studied, since maximum power will be produced at relatively high cycle frequencies. There is a clear trend between species for increased power with increasing temperature and cycle frequency (see Fig. 8 in Stevenson and Josephson, 1990).

Using the estimated *in vivo* strain of  $\pm 3\%$   $l_0$  (Hess and Videler, 1984), power output was almost independent of cycle frequency between 8 and 18Hz, the tailbeat frequency range over which fast fibres are recruited (Fig. 2) (Wardle and Videler, 1993). The *in vitro* simulations therefore suggest that rostral muscle *in vivo* generates near maximum power output over the functionally important tailbeat frequency range. Strain amplitude for maximum power output at 8Hz was  $\pm 5\%$ , not  $\pm 3\%$  (Fig. 2). However, at this low tailbeat frequency, the power demands of swimming will be well below maximum and will be determined to a large extent by the proportion of fast muscle recruited. When the power demand is greatest, at 18Hz, maximum power output was greatest at the strain amplitude estimated for the *in vivo* situation ( $\pm 3\%$ , Fig. 2).

#### *Swimming simulation*

Considering the three points in the body studied, how might these superficial fast muscles (operating in such different ways) act together to contribute to the power required for swimming, accepting the assumption that most of the thrust in carangiform swimming comes from the blade of the caudal fin (Lighthill, 1971; Hess and Videler, 1984)? At the instant when the rostral muscle generates maximum power, activated caudal myotomes reach maximum (Fig. 6) or close to maximum (Fig. 7B) force/stiffness whilst still lengthening. Some of the energy stored by this stretching of active muscle is returned, since, at the onset of the shortening phase of the cycle, the force is higher than it would have been without prestretch and remains higher throughout shortening. (Stretched muscle can maintain forces up to  $1.8P_0$ ; Cavagna *et al.* 1985.) Since work is force multiplied by distance moved, muscle performs more positive work after a prestretch than without it (Fig. 5B). The highest instantaneous power outputs were observed after prestretch of caudal muscle. Rostral muscle therefore appears to act primarily as a power generator, whereas caudal muscle initially acts to transmit this power towards the tail blade, and only as the power output of the rostral muscle declines does the caudal muscle in turn act as the power generator (Fig. 7B).

This sequential recruitment of myotomes as power generators, with the more caudally placed myotomes initially acting to transmit the power towards the tail, is shown clearly in Fig. 7. As instantaneous power output reaches a maximum at 0.35BL, force and stiffness at 0.5/0.65BL approach their maxima. Negative work is performed at both 0.5

---

Fig. 7. (A) Muscle strain and force records of the middle four of eight oscillatory cycles. Records from three preparations, from three fish all of length 29cm, operating under predicted *in vivo* conditions at a cycle frequency of 12Hz. Stimulus phase shift (degrees), number of stimuli and strain ( $\pm\%$   $l_0$ ) were: 30, 2 and 3 (0.35BL); 15, 2 and 4.5 (0.50BL); 330, 1 and 6 (0.65BL). Strain cycles of 0.5BL and 0.65BL preparations lag that of 0.35BL by  $55^\circ$  and  $110^\circ$  respectively, as *in vivo*. The three preparations have different lengths and cross-sectional areas, and force and strain records have not been normalised to account for these differences. Stimulus timing is indicated below the force record for the second cycle. (B) Instantaneous power output over the middle two cycles shown in A. \*Time of peak forces at 0.35BL. †Time of peak force at 0.5/0.65BL. Force at 0.5BL usually peaks slightly earlier than that at 0.65BL. Muscle from 0.35 and 0.50BL performs largely positive work. Positive work at 0.65BL is preceded by a substantial period of negative work production, and mean power output is close to zero.

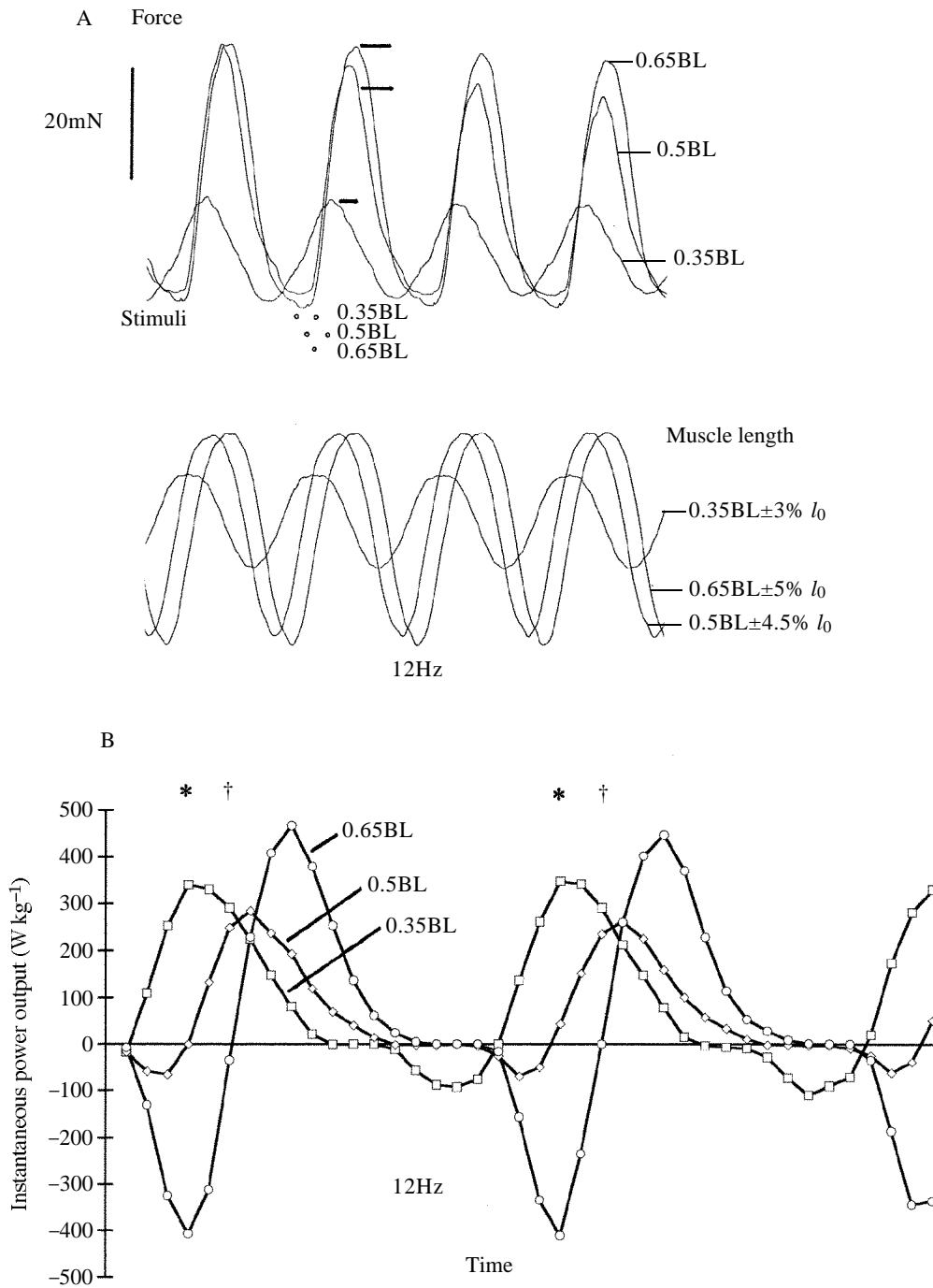
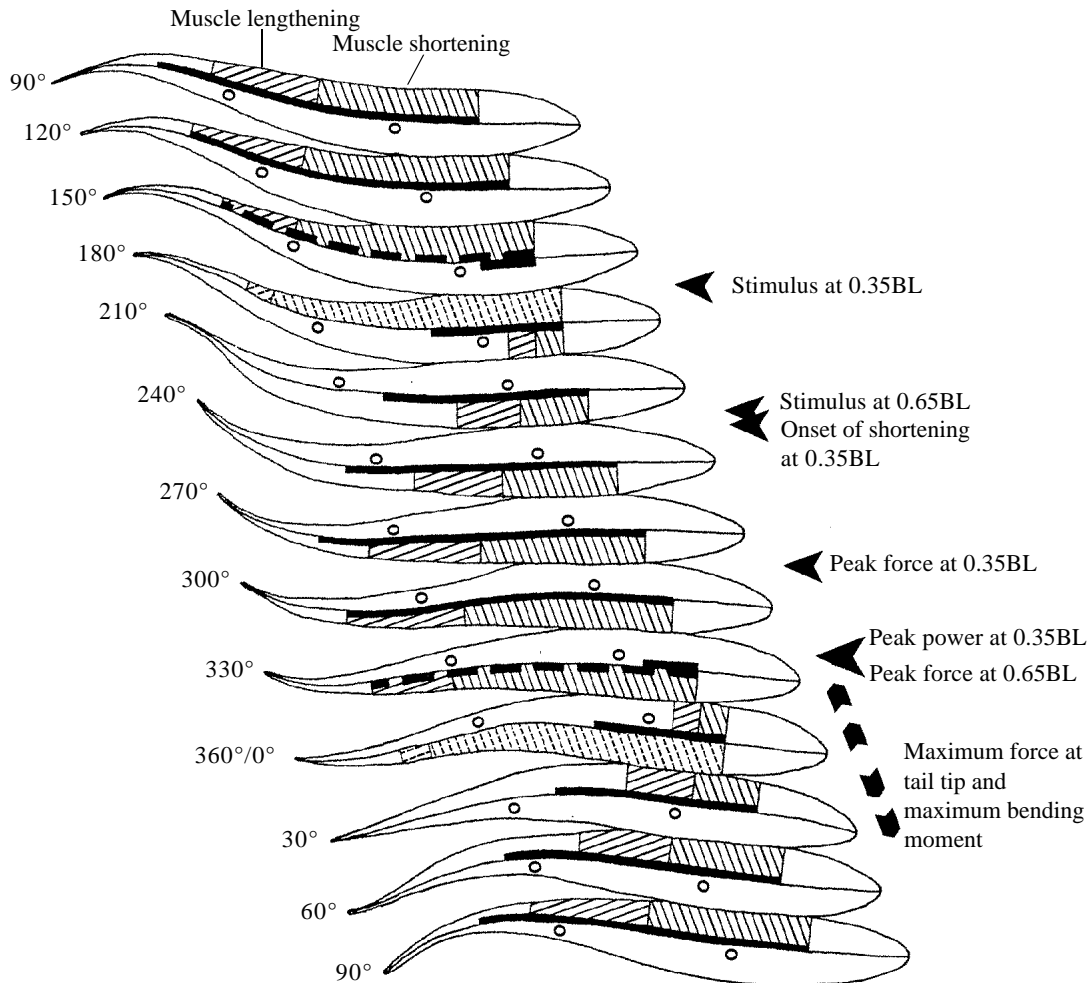


Fig. 7

and 0.65BL as power increases at 0.35BL. As power begins to decline at 0.35BL, power output at 0.5BL becomes positive and rises; it reaches a peak before power at 0.35BL has dropped by 50%. Force at 0.65BL remains high, and the muscle continues to perform negative work as a power transmitter until just before power at 0.50BL peaks. Only then does muscle at 0.65BL perform positive work, with peak positive power output at this location occurring when power output at 0.50BL falls towards 50% of maximum. Muscle at 0.50BL performs only a little negative work in transmitting the power



Phase of muscle strain cycle at tail tip

Fig. 8. A schematic representation of the events of a single tailbeat, showing progressive fish outlines and midlines from above, in 30° increments [fish outlines redrawn from Videler and Hess (1984), with permission]. The more rostral hatched areas indicate muscle active during shortening; the more caudal hatched areas indicate muscle active during lengthening. The thick black line shows the period of EMG activity (0.2-0.8BL); the dashed black line indicates that EMG activity stops at that time. For a detailed explanation see the text.

generated at 0.35BL towards the tail, i.e. there is little active prestretch. At 0.65BL, this force enhancement by stretch (Cavagna *et al.* 1985) is presumably necessary since the lower cross-sectional area of muscle at this location (about 50% of that at 0.35BL, Videler and Hess, 1984) cannot generate the necessary stress by any other means. However, we do not know what role connective tissue may play in this region. Not all of the energy put into the prestretch is lost, for reasons given in the previous paragraph. Despite the high power output over the second half of each active cycle, mean power output over a single tailbeat at 0.65BL is close to zero.

These results show a striking similarity to computer-simulated data published by van Leeuwen *et al.* (1990), based on ciné/EMG recordings of swimming carp and estimated muscle mechanical properties. We noted above that force enhancement by stretch led to a 1.5- to 1.8-fold increase in force in caudal myotomes and a similar increase was predicted by van Leeuwen *et al.* (1990). They also predicted that all myotomes would produce some negative work in the cycle and that it would be small rostrally and increase caudally. At 0.65BL (their point 6, Fig. 6), positive and negative work components are similar and mean power output is close to zero in both studies. Van Leeuwen *et al.* (their Fig. 6) predict that peak negative power can be over twice the magnitude of peak positive power, in accordance with our own findings (data not shown). It should be stressed that, in both studies, muscle strain has been calculated from deformations of the body and awaits confirmation by more direct methods. However, these are not without their own problems – the presence of even fine EMG electrodes can lead to changes in swimming movements, increasing muscle strain twofold (van Leeuwen *et al.* 1990), and direct measurements using techniques such as sonomicrometry must be carefully applied.

Fig. 8 shows a schematic representation of the events of a single tailbeat, based on our own data and results from previous studies (Hess and Videler, 1984; van Leeuwen *et al.* 1990; Wardle and Videler, 1993). The figure shows progressive fish outlines and midlines

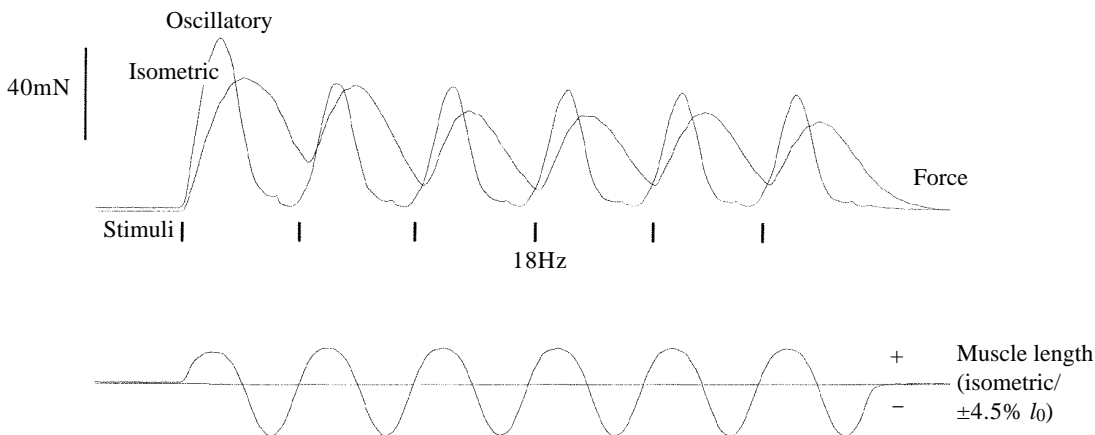


Fig. 9. Single supramaximal stimuli given at 18Hz, under isometric conditions and during imposed sinusoidal strains (stimulus phase shift  $0^\circ$ ), for a mid-point (0.5BL) preparation. The imposition of sinusoidal strains decreases time to peak force and relaxation time and reduces force between stimuli.

from above through one complete tailbeat cycle, in 30° increments. The phase value on the left of each fish refers to the muscle strain phase at the tail tip. The period of EMG activity between 0.2 and 0.8BL is shown by the thick black line on either side of the midline (from Wardle and Videler, 1993). The dashed line indicates that EMG activity stops at that moment. EMG activity occupies the same phase and relative duration within a tailbeat at all swimming speeds (Wardle and Videler, 1993). The hatched areas indicate that segment of the superficial fast muscle generating more than 50% of the maximum force developed in the cycle, for a fish swimming at 18Hz. The lengths of these segments were calculated from experiments similar to those in Figs 5–7. They vary minimally with frequency and do not affect the basic description. The more rostral hatched areas indicate shortening muscle operating in the ‘power phase’ – generating a large, positive mean power output. Caudally placed hatched areas indicate muscle operating in its ‘transmission phase’ – that is, active during lengthening, generating large forces and transmitting the power generated by more rostral muscle towards the tail. Partial hatching is shown where the muscle force is falling below 50% of maximum. The description is based on estimated *in vivo* events at locations 0.35 and 0.65BL from the head (indicated by the small open circles in the fish profiles), predicted *in vivo* events at 0.50BL and the known mechanical properties of the muscle at these locations. For comparison with the isolated muscle experiments at 18Hz (Figs 5 and 6), the timings of muscle stimuli, peak forces and the transition from shortening to lengthening are given. The predicted time of maximum tail blade force and maximum bending moment (Lighthill, 1971; Hess and Videler, 1984; Tang and Wardle, 1992) is indicated as a broad zone around 360°/0°.

Early in the rightward tail sweep (tail tip phase 180°), power is generated by the most rostral right-side myotomes, and this power is transmitted towards the tail blade by stiffened myotomes placed more caudally. Because of the phase differences between the caudally travelling waves of muscle activation and bending (Hess and Videler, 1984; van Leeuwen *et al.* 1990; Wardle and Videler, 1993), there is a change in muscle function along the length of the body. Rostrally, active muscle shortens and generates power; caudally, active muscle stiffens, resisting stretch, for the transmission of this power to the tail blade. A transition zone, in which the muscle’s role switches from power transmitter to power generator, travels caudally during the tailbeat. Travelling from head to tail, myotomes spend an increasing proportion of the early phase of the tailbeat transmitting forces caudally, generating power over progressively later and shorter phases of the cycle, as the tail blade completes its cycle (Fig. 8). All but the most caudal myotomes contribute to the movement of the tail, with a power-generating phase towards the end of the tailbeat.

Maximum tailbeat frequency will be determined largely by the rate at which rostral myotomes can do work, hence the short contraction time. It will be interesting to compare the results with those of deeper fast fibres, which operate under rather different constraints (Alexander, 1969; Rome and Sosnicki, 1991). Caudal myotomes are switched off for most of the tailbeat (van Leeuwen *et al.* 1990; Wardle and Videler, 1993), but their longer contraction time ensures that force is high late in the cycle and positive work is performed. If it is assumed that  $t_{90}$  gives an approximate measure of the minimal cycle time, and therefore the maximum rate at which the muscle can perform net positive work,

then for this size of saithe at 12°C, tailbeat frequencies of 16 and 8Hz are predicted from the  $t_{90}$  of rostral (62ms) and caudal (134ms) muscles. However, the imposed strain cycle has a dramatic effect on the mechanical response (Fig. 9), decreasing apparent contraction time and increasing the frequency range over which muscle can function, either to generate or to transmit power. In both cases, force must be close to zero over some part of the tailbeat cycle.

The hypothesised transmission of muscle power down the body to the tail is consistent with accepted theories on swimming, which show that thrust is developed largely at the tail blade (Lighthill, 1971). Maximum force is measured at the tail blade as it crosses the swimming track (Lighthill, 1971; Tang and Wardle, 1992), and this coincides with the incident of maximum bending moment all along the body (Hess and Videler, 1984). At much the same instant, rostral muscle generates its maximum power output and the caudal muscle its maximum force (Figs 5–8). The small discrepancy between the timing of maximum bending moment and peak power/force at 0.35/0.65BL may be due to the fish outlines used. These were taken from a real fish, which was not swimming with exactly uniform speed and tailbeat frequency. Rostral myotomes, as observed (Fig. 5–7), should generate peak force before caudal myotomes because of the inertial forces in the caudal part of the body as it reverses its direction of lateral movement.

Why is muscle rather than tendon used to transmit power in the caudal region? Our description of events refers to swimming at constant tailbeat frequency in a straight line. In life, fish spend much of their time starting, stopping, accelerating, decelerating and changing direction. Under these conditions, the muscle has different roles. Furthermore, the muscle is only acting as a transmission element for part of the tailbeat cycle: for much of the rest of it, it is generating power (Fig. 7B). In some tuna, part of the caudal musculature has been replaced by tendons (Kishinouye, 1923), but thunniform swimmers have a more rigid body and are less manoeuvrable. It is likely that the myotomal muscle operates under somewhat different conditions from those of the carangiform saithe.

J.D.A. gratefully acknowledges the support of the Royal Society. We would like to thank Iain Young, Professor R. McNeill Alexander and Professor Sir Eric J. Denton for many useful discussions. We also thank Alistair Johnstone for his support and single malts at the field station.

### References

- ALEXANDER, R. McN. (1969). The orientation of muscle fibres in the myomeres of fishes. *J. mar. biol. Ass. U.K.* **49**, 263–290.
- ALTRINGHAM, J. D. AND JOHNSTON, I. A. (1990a). Modelling muscle power output in a swimming fish. *J. exp. Biol.* **148**, 395–402.
- ALTRINGHAM, J. D. AND JOHNSTON, I. A. (1990b). Scaling effects in muscle function: power output of isolated fish muscle fibres performing oscillatory work. *J. exp. Biol.* **151**, 453–467.
- CAVAGNA, G. A., MAZZANTI, M., HEGLUND, N. C. AND CITTERIO, G. (1985). Storage and release of mechanical energy by active muscle: a non-elastic mechanism. *J. exp. Biol.* **115**, 79–87.
- HESS, F. AND VIDELER, J. J. (1984). Fast continuous swimming of saithe (*Pollachius virens*): a dynamic analysis of bending moments and muscle power. *J. exp. Biol.* **109**, 229–251.

- JOHNSTON, I. A. AND MOON, T. W. (1980). Endurance exercise training in the fast and slow muscles of a teleost fish, *Pollachius virens*. *J. comp. Physiol.* **135**, 147–156.
- JOSEPHSON, R. K. (1985). Mechanical power output from striated muscle during cyclic contractions. *J. exp. Biol.* **114**, 493–512.
- KISHINOUE, K. (1923). Contributions to the comparative study of the so-called scombroid fishes. *J. Coll. Agric. imp. Univ. Tokyo* **8**, 295–473.
- LIGHTHILL, M. J. (1971). Large-amplitude elongated-body theory of fish locomotion. *Proc. R. Soc. Lond. B* **179**, 125–138.
- MOON, T. W., ALTRINGHAM, J. D. AND JOHNSTON, I. A. (1991). Energetics and power output of isolated, fish fast muscle fibres performing oscillatory work. *J. exp. Biol.* **158**, 261–273.
- ROME, L. C. AND SOSNICKI, A. A. (1991). Myofilament overlap in swimming carp. II. Sarcomere length changes during swimming. *Am. J. Physiol.* **260**, C289–C296.
- STEVENSON, R. D. AND JOSEPHSON, R. K. (1990). Effects of operating frequency and temperature on mechanical power output from moth flight muscle. *J. exp. Biol.* **149**, 61–78.
- TANG, J. AND WARDLE, C. S. (1992). Power output of two sizes of Atlantic salmon (*Salmo salar*) at their maximum sustained swimming speeds. *J. exp. Biol.* **166**, 33–46.
- VAN LEEUWEN, J. L., LANKHEET, M. J. M., AKSTER, H. A. AND OSSE, J. W. M. (1990). Function of red axial muscles of carp (*Cyprinus carpio* L.): recruitment and normalised power output during swimming in different modes. *J. Zool., Lond.* **220**, 123–145.
- VIDELER, J. J. AND HESS, F. (1984). Fast continuous swimming of two pelagic predators, saithe (*Pollachius virens*) and mackerel (*Scomber scombrus*): a kinematic analysis. *J. exp. Biol.* **109**, 209–228.
- WARDLE, C. S., VIDELER, J. J., ARIMOTO, T., FRANCO, J. M. AND HE, P. (1989). The muscle twitch and the maximum swimming speed of the giant bluefin tuna, *Thunnus thynnus* L. *J. Fish Biol.* **35**, 129–137.
- WARDLE, C. S. (1985). Swimming activity in marine fish. In *Physiological Adaptations of Marine Animals* (ed. M. S. Laverack), pp. 521–540. Cambridge: Company of Biologists.
- WARDLE, C. S. AND VIDELER, J. J. (1993). The timing of the emg in the lateral myotomes of mackerel and saithe at different swimming speeds. *J. Fish Biol.* **42**, 347–359.
- WILLIAMS, T. L., GRILLNER, S., SMOLJANINOV, V. V., WALLÉN, P., KASHIN, S. AND ROSSIGNOL, S. (1989). Locomotion in lamprey and trout: the relative timing of activation and movement. *J. exp. Biol.* **143**, 559–566.